



doi: 10.31648/ts.4996

## AN ANALYSIS OF NON-ISOTHERMAL PRIMARY CRYSTALLIZATION KINETICS OF $\text{Fe}_{95}\text{Si}_5$ AMORPHOUS ALLOY

*Adam Frączyk<sup>1</sup>, Krzysztof Kuś<sup>2</sup>, Adam Wojtkowiak<sup>3</sup>*

<sup>1</sup>ORCID: 0000-0002-3056-3141

Department of Material and Machine Technology  
University of Warmia and Mazury in Olsztyn

<sup>2</sup>ORCID: 0000-0001-9811-5831

Department of Material and Machine Technology  
University of Warmia and Mazury in Olsztyn

<sup>3</sup>Department of Material and Machine Technology  
University of Warmia and Mazury in Olsztyn

Received 7 October 2019, accepted 26 January 2020, available online 27 January 2020.

**Key words:** metallic glass, energy activation, Avrami exponent, crystallization kinetics parameter, DSC.

### Abstract

The paper describes the primary crystallization of metallic  $\text{Fe}_{95}\text{Si}_5$  glass which was studied by differential scanning calorimetry (DSC) with non-isothermal methods. The activation energy of crystal transformation was calculated with the equations proposed by Kissinger, Mahadevan and a modified version of the equation developed by Augis and Bennett. Activation energy was determined at  $E_a = 242.0 - 254.2$  kJ / mol, subject to the applied method. The Avrami exponent of crystallization in the amorphous phase  $n$  was determined in the range of  $n = 2.40 - 2.52$ , depending on the method of calculating the transformation of activation energy.

## Introduction

Amorphous alloys, also known as metallic glass, have numerous industrial applications due to their excellent soft magnetic properties. The properties of amorphous alloys continue to be investigated (LI et al. 2008, SAHINGOZA et al. 2004, NOBUYUKI et al. 2007).

Thermal treatment and nanocrystallization improve the properties of metallic glass. The crystallization of amorphous alloys can be controlled, which is particularly important consideration in the production of materials with a specific structure. These processes require a thorough understanding of the crystallization kinetics of metallic glass.

The crystallization kinetics of chalcogenide glass can be analyzed by isothermal and non-isothermal methods, and the results can be interpreted with the use of several theoretical models (KISSINGER 1957, OZAWA 1970, MATUSITA et al. 1979, MATUSITA et al. 1980, KONG et al. 2011, REZAEI-SHAHREZA et al. 2017). In recent years, new isoconversional methods have been applied to determine the crystallization parameters of amorphous alloys during non-isothermal heating (REZAEI-SHAHREZA et al. 2017, ANSARINIYA et al. 2018, JAAFARI et al. 2018).

Isothermal analyses involve the JMA equation which is a primary method for determining crystallization parameters. However, non-isothermal techniques have also been used in numerous experiments. Different values of crystallization kinetic parameters were reported in Fe-based amorphous alloys. For example, the estimated values of the Avrami exponent ranged from 1.0 to 4.0 (GIBSON et al. 1987, SANTOS et al. 2002). The activation energy of the same alloy can also be calculated with the use of different models and equations. The aim of the present study was to determine the activation energy of the primary crystallization process based on the equations proposed by Kissinger and Mahadevan and the modified version of the equation developed by Augis and Bennett. The Avrami exponent of crystallization kinetics  $n$  which describes the mechanism of crystalline phase formation was also calculated.

## Theory

The analyses of the crystallization kinetics of amorphous alloys generally involve two parameters: activation energy  $E_a$  and the Avrami exponent of crystallization kinetics  $n$ .

Both isothermal and non-isothermal methods can be used in calorimetric measurements. Most methods rely on the Johnson-Mehl-Avrami-Kolmogorov (JMAK) equation of isothermal transformation kinetics (MÁLEK 2000, WANG et al. 2014):

$$x(t) = 1 - \exp(-Kt^n) \quad (1)$$

where:

- $x(t)$  – volume fraction transformed after time  $t$ ,
- $n$  – the Avrami exponent which reflects the nucleation rate and the growth morphology,
- $K$  – the reaction rate constant.

The temperature dependence of the reaction rate is usually determined with the use of the Arrhenius equation:

$$K = K_0 \exp\left(\frac{-E_a}{RT}\right) \tag{2}$$

where:

- $E_a$  – the activation energy for the crystallization reaction,
- $K_0$  – the frequency factor,
- $R$  – the gas constant.

Non-isothermal crystallization is characterized by a constant heating rate. The relationship between sample temperature  $T$  and heating rate  $\beta$  can be expressed by the following equation:

$$T = T_0 + \beta t \tag{3}$$

The activation energy of primary crystallization can be determined using the models developed by Kissinger (KISSINGER 1957), Ozawa (OZAWA 1970), Mahadevan (MAHADEVAN et al. 1986) and Augis-Bennett (AUGIS et al. 1978). These methods are based on the JMAK theory (Eq. 1) and the logarithmic form of Equation 2. These models account for the fact that the volume of the crystallized fraction at the top of the crystallization peak in DSC is  $x_p=0.63$ . When the highest rate of transformation is applied at maximum peak approximations, the relevant equations can be interpreted as follows:

a) Kissinger model

$$\ln\left(\frac{\beta}{T_p^2}\right) = \frac{-E_a}{RT_p} + \ln\left(\frac{K_0 R}{E_a}\right) \tag{4}$$

b) Mahadevan model

$$\ln(\beta) = \frac{-E_a}{RT_p} + \ln\left(\frac{K_0 E_a}{R}\right) \tag{5}$$

c) Modified version of the Augis and Bennett model

$$\ln\left(\frac{\beta}{T_p}\right) = \frac{-E_a}{RT_p} + \ln(K_0) \tag{6}$$

where:

- $T_p$  – peak temperature,
- $\beta=dT/dt$  – the heating rate.

The partial values of  $\ln(K_0R/E_a)$ ,  $\ln(K_0E_a/R)$  and  $\ln(K_0)$  in Equations 4, 5 and 6 are constant. From it is possible to derive The value of activation energy  $E_a$  and pre-exponential factor  $K_0$  of the crystallization process can be derived from the slope and the intercept of the straight line (Equations 4, 5, 6), respectively.

The Avrami exponent  $n$  is also an important crystallization parameter, and it can be determined with the use of various methods. In the model developed by Ozawa, time in Equation 1 was replaced by temperature in Equation 3 to produce the following equation:

$$x(t) = 1 - \exp \left[ - \left\{ \frac{K(T - T_0)}{\beta} \right\} \right] \quad (7)$$

Double logarithmic transformation can be applied to produce the following equation:

$$\ln[-\ln(1 - x)] = -n \ln(\beta) + n \ln(T - T_0) \quad (8)$$

The values of  $\ln[-\ln(1 - x)]$  are plotted against  $\ln(\beta)$  from various DSC thermograms, and the Avrami exponent  $n$  is derived from the slope of the straight line (Eq. 8). The Avrami exponent  $n$  can also be determined with the following equation (GAO et al. 1986, JAKUBCZYK et al. 2008):

$$n = \left( \frac{dx}{dt} \right)_p RT_p^2 (0,37\beta E_a)^{-1} \quad (9)$$

where:

$(dx/dt)_p$  – the maximum crystallization rate.

## Experimental

Amorphous samples were obtained by rapid solidification of melts using the melt-spinning method (Fig. 1). The obtained ribbon was 20 mm wide and 0.03 mm thick. The nominal composition of  $\text{Fe}_{95}\text{Si}_5$  is presented in Figure 2.

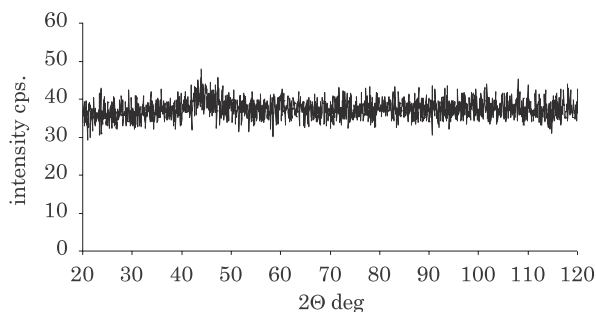


Fig. 1. XRD pattern of  $\text{Fe}_{95}\text{Si}_5$  amorphous alloy

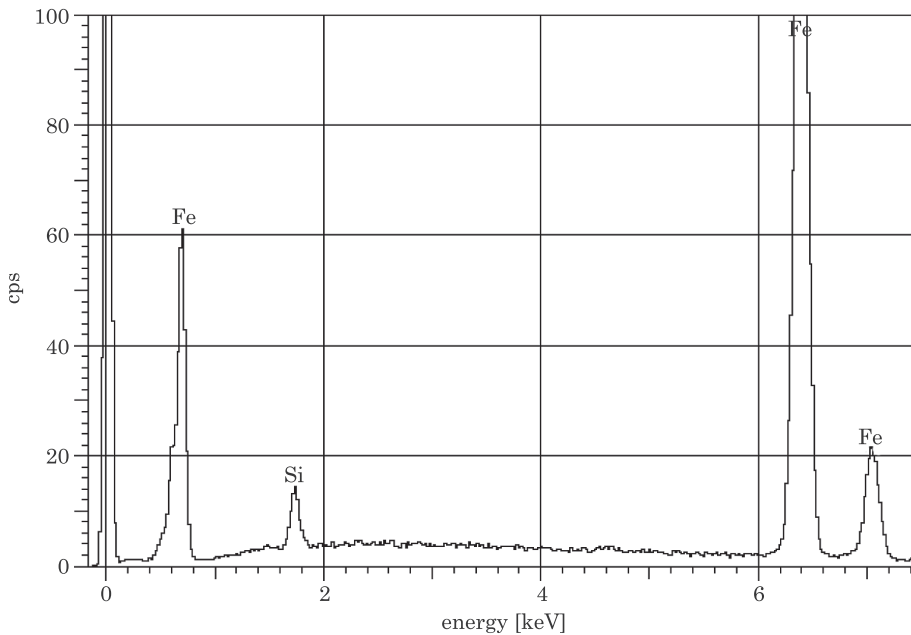


Fig. 2. EDS spectrum of  $Fe_{95}Si_5$  amorphous alloy

The crystallization process was investigated by differential scanning calorimetry (DSC) in a nitrogen atmosphere using the Netzsch DSC 204 differential scanning calorimeter. Temperature and energy calibrations were performed based on the melting temperatures and melting enthalpies of high-purity zinc and indium registered in the device. Sample mass in DSC measurements approximated several milligrams. The samples were heated from 340 K to 840 K at different heating rates ( $\beta = 5, 10, 20$  and  $30 \text{ K min}^{-1}$ ).

## Results and Discussion

The DSC thermograms for the crystallization of  $Fe_{95}Si_5$  at various heating rates are presented in Figure 3. The two crystallization peaks of  $Fe_{95}Si_5$  involve two resolved phase transformations. The position of both peaks shifted to higher temperatures with an increase in heating rate. The first peak corresponds to phase formation in  $\alpha\text{-Fe(Si)}$  (FRĄCZYK 2011). The observed shift of the onset of crystallization  $T_x$  to higher temperatures is the result of the induction time of the nucleation process. There is a nucleation time during crystallization. When the heating rate increases, the onset of crystallization shifts to higher temperatures.

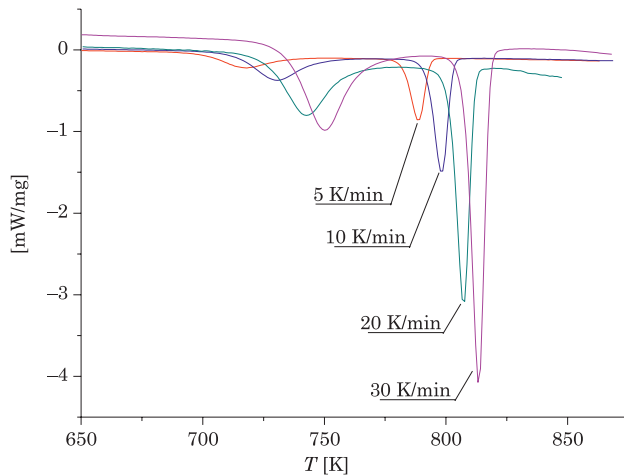


Fig. 3. DSC curves of  $\text{Fe}_{95}\text{Si}_5$  for several heating rates illustrating primary crystallization (first peak) and secondary crystallization (second peak) processes

The activation energy  $E_a$  of the primary crystallization of  $\text{Fe}_{95}\text{Si}_5$  metallic glass was calculated with the use of the models proposed by Kissinger and Mahadevan and the modified version of the Augis and Bennett model (4-6). For this purpose, the values of  $\ln(\beta/T_p^2)$  vs.  $10^3/T_p$  (Fig. 4),  $\ln(\beta)$  vs.  $10^3/T_p$  (Fig. 5) and  $\ln(\beta/T_p^2)$  vs.  $10^3/T_p$  (Fig. 6) were plotted for the amorphous alloy.

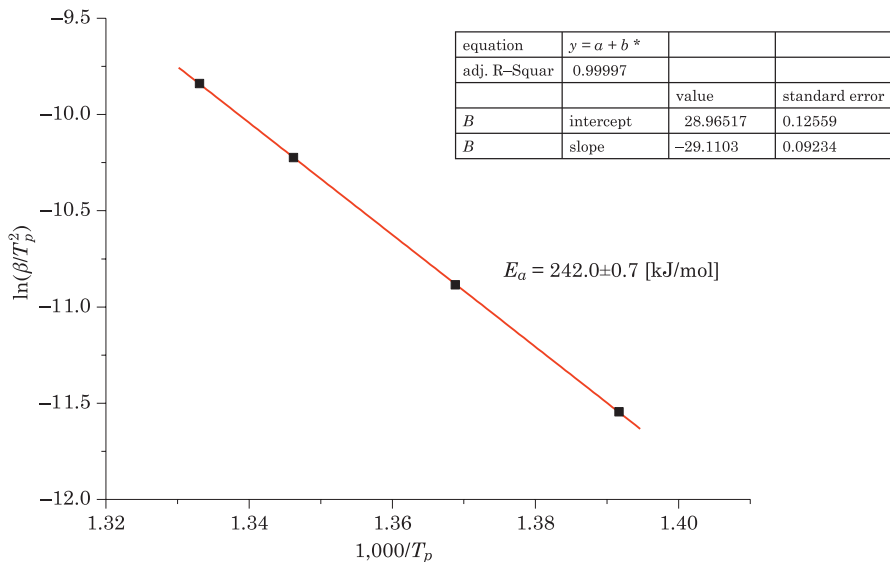


Fig. 4. Plot of  $\ln(\beta/T_p^2)$  vs  $1,000/T_p$  values for the determination of activation energy  $E_a$  from a set of DSC scans with different heating rates (5, 10, 20 and 30 K/min). The analysis was performed for the first exothermic DSC reaction of  $\text{Fe}_{95}\text{Si}_5$  amorphous alloy

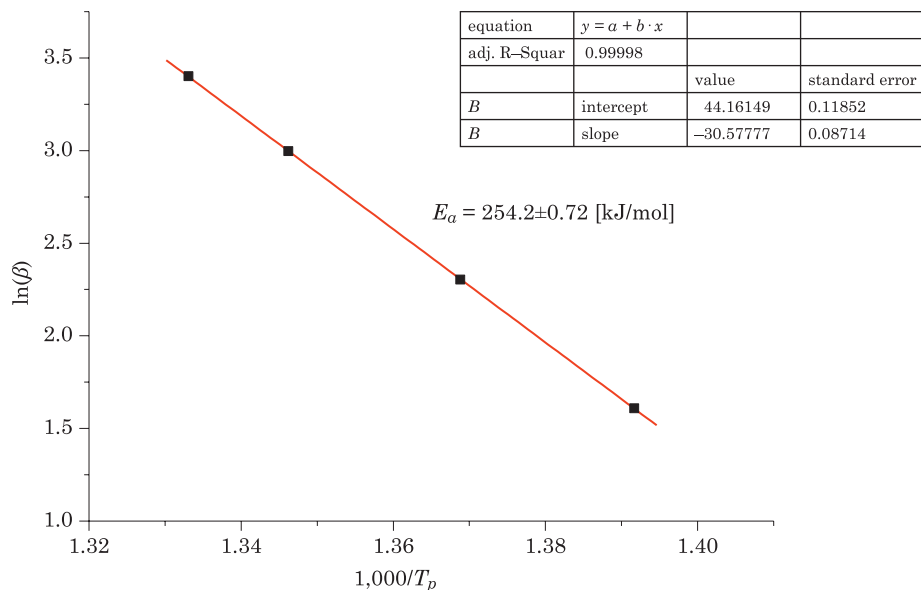


Fig. 5. Plot of  $\ln(\beta)$  vs  $1,000/T_p$  values for the determination of activation energy  $E_a$  from a set of DSC scans with different heating rates (5, 10, 20 and 30 K/min). The analysis was performed for the first exothermic DSC reaction of  $Fe_{95}Si_5$  amorphous alloy

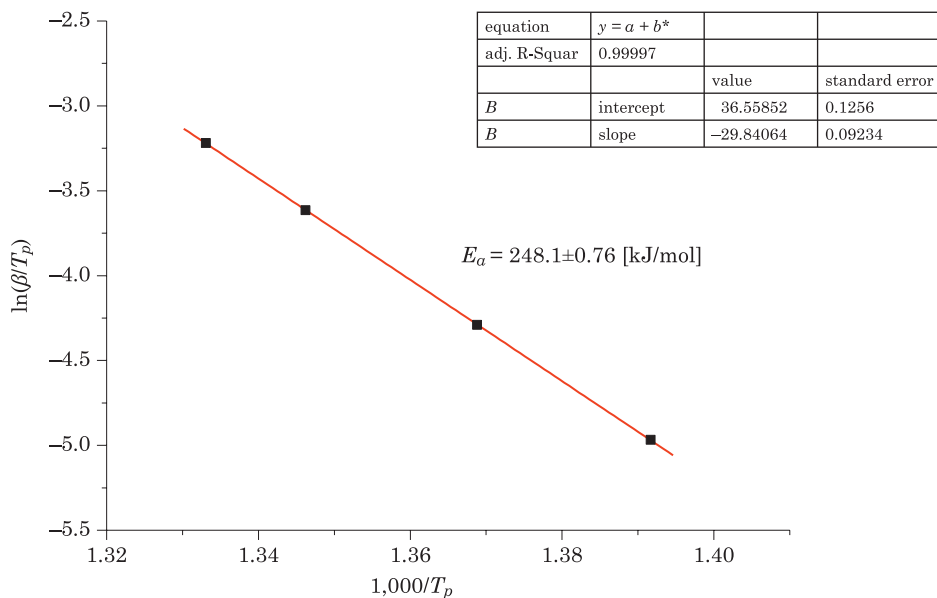


Fig. 6. Plot of  $\ln(\beta/T_p)$  vs  $1,000/T_p$  values for the determination of activation energy  $E_a$  from a set of DSC scans with different heating rates (5, 10, 20 and 30 K/min). The analysis was performed for the first exothermic DSC reaction of  $Fe_{95}Si_5$  amorphous alloy

The activation energy  $E_a$  of an amorphous alloy can be derived from the slope ( $-E_a/R$ ) of the line. The line of best fit was determined with the least squares method. The arithmetic mean and standard deviation were calculated for activation energies. The results are presented in Table 1.

Table 1

Parameters of primary crystallization kinetics of $\text{Fe}_{95}\text{Si}_5$ metallic glass			
Parameter	Kissinger equation	Mahadevan equation	Modified version of the Augis & Bennett equation
$Ea$ [kJ/mol]	242.0	254.2	248.1
$N$	2.52	2.46	2.40

The crystallized fraction  $x$  at temperature  $T$  was expressed as  $x(T) = Ax(T)/A$ , where  $A$  and  $Ax$  represent the total area and the partial area (at generic temperature  $T$ ) of the exothermic peak, respectively. The relationship between the crystallized volume fraction and the time of the first exothermic peak of amorphous  $\text{Fe}_{95}\text{Si}_5$  alloy is presented in Figure 7.

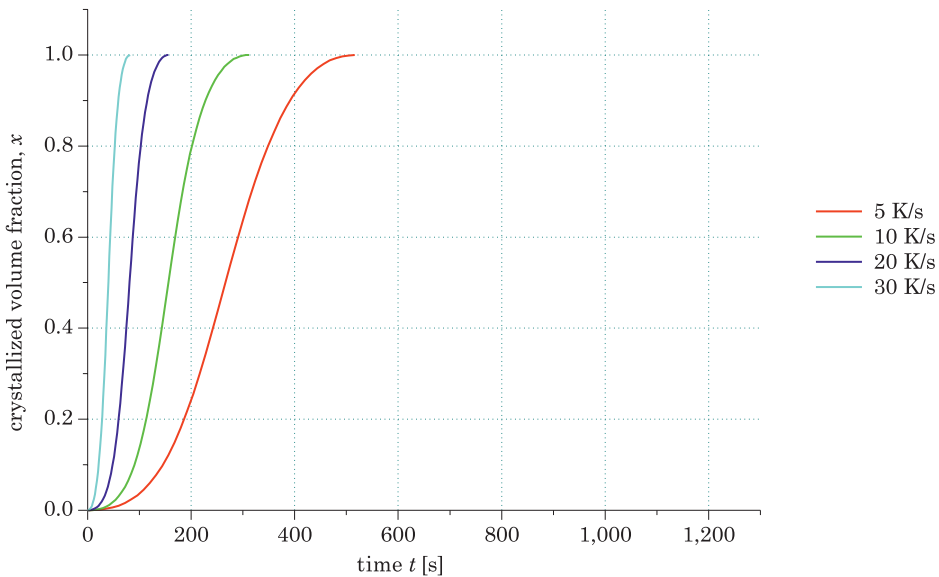


Fig. 7. Crystallized volume fraction  $x$  as a function of time  $t$  for  $\text{Fe}_{95}\text{Si}_5$  metallic glass at different heating rates  $\beta$



In Figure 8, the data from Figure 5 were expressed as a function of time  $t$  to illustrate the relationship between crystallization rate  $dx/dt$  and temperature  $T$ .

The Avrami exponent  $n$  was calculated by substituting the maximum value of  $dx/dt$  into Equation 9 for different heating rates. The primary crystallization parameters are presented in Table 1.

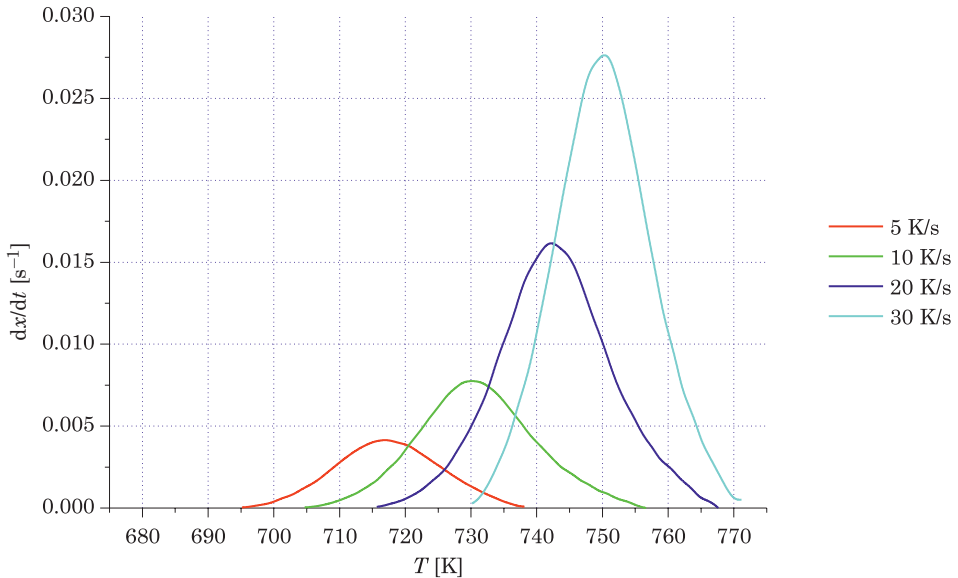


Fig. 8. Curve of crystallization rate  $dx/dt$  vs temperature  $T$  for  $\text{Fe}_{95}\text{Si}_5$  amorphous alloy at different heating rates  $\beta$

Activation energy  $E_a$  and the Avrami exponent  $n$  are the most important kinetic parameters describing the crystallization of amorphous alloys. The highest activation energy  $E_a$  was obtained with the Mahadevan equation (Equation 5), and the lowest activation energy was obtained with the Kissinger equation (Equation 4). The extreme values of  $E_a$  differed by nearly 5%.

Similar results were reported by AL-HENITI (2009) in an analysis of the crystallization kinetics of  $\text{Fe}_{78}\text{Ni}_{1.5}\text{Si}_9\text{B}_3$  metallic glass.

## Conclusions

The values of activation energy and the Avrami exponent  $n$ , which are associated with the first peak temperature in continuous heating DSC curves of amorphous  $\text{Fe}_{95}\text{Si}_5$  alloy, were estimated with the use of acclaimed methods.

The values of Avrami exponent  $n$  indicate that during the first stages of the crystallization process a crystal growth controlled respectively by diffusion and by interface takes place.

In order compare the activation energy of different amorphous alloys the same equation or model should be applied.

## References

- AL-HENITI S.H. 2009. *Kinetic study of non-isothermal crystallization in  $Fe_{78}Si_9B_{13}$  metallic glass*. Journal of Alloys and Compounds, 484: 177–184.
- ANSARINIYA M., SEIFODDINI A., HASANI S. 2018. *( $Fe_{0.9}Ni_{0.1}$ ) $_{77}Mo_5P_9C_{7.5}B_{1.5}$  bulk metallic glass matrix composite produced by partial crystallization: The non-isothermal kinetic analysis*. Journal of Alloys and Compounds, 763: 606–612.
- AUGIS J.A., BENNTT J.E. 1978. *Calculation of the Avrami Parameters for Heterogeneous Solid State Reactions Using a Modification of the Kissinger Method*. Journal of Thermal Analysis, 13: 283–292.
- FRĄCZYK A. 2011. *The activation energy of primary crystallization of  $Fe_{95}Si_5$  metallic glass*. Technical Science, 14(1): 93–100.
- GAO Y.Q., WANG W. 1986. *On the activation energy of crystallization in metallic glasses*. Journal of Non-Crystalline Solids, 81: 129–134.
- GIBSON M.A., DELAMORE G.W. 1987. *Crystallization kinetics of some iron-based metallic glasses*. Journal of Material Science, 22(12): 4550–4557.
- JAKUBCZYK E., KRAJCZYK A., JAKUBCZYK M. 2008. *Crystallization of amorphous  $Fe_{78}Si_9B_{13}$  alloy*. Journal of Physics: Conference Series, 79: 012008.
- JUNG H. Y., STOICA M., YI S., KIM D.H., ECKERT J. 2015. *Crystallization Kinetics of  $Fe_{76.5-x}C_{6.0}Si_{3.3}B_{5.5}P_{8.7}Cu_x$  ( $x = 0, 0.5, \text{ and } 1 \text{ at. pct}$ ) Bulk Amorphous Alloy*. Metallurgical and Materials Transactions, 46(A): 2415–2421.
- JAAFARI Z., SEIFODDINI A., HASANI S., REZAEI-SHAHREZA P. 2018. *Kinetic analysis of crystallization process in [ $(Fe_{0.9}Ni_{0.1})_{77}Mo_5P_9C_{7.5}B_{1.5}$ ] $_{100-x}Cu_x$  ( $x = 0.1 \text{ at. \%}$ ) BMG*. Journal of Thermal Analysis and Calorimetry, 134: 1565–1574.
- KISSINGER H. E. 1957. *Reaction kinetics in differential thermal analysis*. Analytical Chemistry, 29: 1702–1706.
- KONG L.H., GAO Y.L., SONG T.T., WANG G., ZHAI Q. J. 2011. *Non-isothermal crystallization kinetics of  $FeZrB$  amorphous alloy*. Thermochemica Acta, 522: 166–172.
- LI H.X., JUNG H.Y., YI S. 2008. *Glass forming ability and magnetic properties of bulk metallic glasses  $Fe_{68.7-x}C_{7.0}Si_{3.3}B_{5.5}P_{8.7}Cr_{2.3}Mo_{2.5}Al_{2.0}Co_x$  ( $x = 0-10$ )*. Journal of Magnetism and Magnetic Materials, 320: 241–245.
- MAHADEVAN S., GIRIDHAR A., SINGH A.K. 1986. *Calorimetric measurements on as-sb-se glasses*. Journal of Non-Crystalline Solids, 88(1): 11–34.
- MÁLEK J. 2000. *Kinetic analysis of crystallization processes in amorphous materials*. Thermochemica Acta, 355: 239–253.
- MATUSITA K, SAKKA S. 1979. *Kinetic Study of the Crystallisation of Glass by Differential Scanning Calorimetry*. Physics and Chemistry of Glasses, 20: 81–84.
- MATUSITA K, SAKKA S. 1980. *Kinetic study of crystallization of glass by differential thermal analysis-criterion on application of Kissinger plot*. Journal of Non-Crystalline Solids, 38–39(2): 741–746.
- NOBUYUKI N., KENJI A., AKIHISA I. 2007. *Novel applications of bulk metallic glass for industrial products*. Journal of Non-Crystalline Solids, 353: 3615–3621.
- OZAWA T. 1970. *Kinetic analysis of derivative curves in thermal analysis*. Journal of Thermal Analysis, 2: 301–324.

- REZAEI-SHAHREZA P., SEIFODDINI A., HASANI S. 2017. *Thermal stability and crystallization process in a Fe-based bulk amorphous alloy: The kinetic analysis*. Journal of Non-Crystalline Solids, 471: 286–294.
- REZAEI-SHAHREZA P., SEIFODDINI A., HASANI S. 2017. *Non-isothermal kinetic analysis of nano-crystallization process in (Fe<sub>41</sub>Co<sub>7</sub>Cr<sub>15</sub>Mo<sub>14</sub>Y<sub>2</sub>C<sub>15</sub>)<sub>94</sub>B<sub>6</sub> amorphous alloy*. Thermochimica Acta, 652: 119–125.
- SAHINGOZA R., EROLA M., GIBBS M.R.J. 2004. *Observation of changing of magnetic properties and microstructure of metallic glass Fe<sub>78</sub>Si<sub>9</sub>B<sub>13</sub> with annealing*. Journal of Magnetism and Magnetic Materials, 271: 74–78.
- SANTOS D.S., SANTOS D.R., BIASI R.S. 2002. *Study of crystallization in the Fe<sub>86</sub>Cu<sub>1</sub>Zr<sub>7</sub>B<sub>6</sub> amorphous alloy using FMR and DSC*. Journal of Magnetism and Magnetic Materials, 242–245(2): 882–884.
- WANG T., YANG X., LI Q. 2014. *Effect of Cu and Nb additions on crystallization kinetics of Fe<sub>80</sub>P<sub>13</sub>C<sub>7</sub> bulk metallic glasses*. Thermochimica Acta, 579: 9–14.

